Shock-Tube Study of the Thermal Decomposition of CH_3CHO and $CH_3CHO + H$ Reaction

Tobias Bentz, Frank Striebel,† and Matthias Olzmann*

Institut für Physikalische Chemie, Universität Karlsruhe (TH), Kaiserstrasse 12, 76128 Karlsruhe, Germany

Received: March 7, 2008; Revised Manuscript Received: April 2, 2008

The thermal decomposition of acetaldehyde, $CH_3CHO + M \rightarrow CH_3 + HCO + M$ (eq 1), and the reaction $CH_3CHO + H \rightarrow$ products (eq 6) have been studied behind reflected shock waves with argon as the bath gas and using H-atom resonance absorption spectrometry as the detection technique. To suppress consecutive bimolecular reactions, the initial concentrations were kept low ($\sim 10^{13}$ cm^{-3}). Reaction 1 was investigated at temperatures ranging from 1250 to 1650 K at pressures between 1 and 5 bar. The rate coefficients were determined from the initial slope of the hydrogen profile via $k_1 = [CH_3CHO]_0^{-1} \times d[H]/dt$, and the temperature dependences observed can be expressed by the following Arrhenius equations: $k_1(T, 1.4\ \text{bar}) = 2.9 \times 10^{14} \exp(-38\ 120\ \text{K}/T)\ \text{s}^{-1}$, $k_1(T, 2.9\ \text{bar}) = 2.8 \times 10^{14} \exp(-37\ 170\ \text{K}/T)\ \text{s}^{-1}$, and $k_1(T, 4.5\ \text{bar}) = 1.1 \times 10^{14} \exp(-35\ 150\ \text{K}/T)\ \text{s}^{-1}$. Reaction 6 was studied with C_2H_5I as the H-atom precursor under pseudo-first-order conditions with respect to CH_3CHO in the temperature range 1040−1240 K at a pressure of 1.4 bar. For the temperature dependence of the rate coefficient the following Arrhenius equation was obtained: $k_6(T) = 2.6 \times 10^{-10} \exp(-3470\ \text{K}/T)\ \text{cm}^3\ \text{s}^{-1}$. Combining our results with low-temperature data published by other authors, we recommend the following expression for the temperature range 300−2000 K: $k_6(T) = 6.6 \times 10^{-18} (T/\text{K})^{2.15} \exp(-800\ \text{K}/T)\ \text{cm}^3\ \text{s}^{-1}$. The uncertainties of the rate coefficients k_1 and k_6 were estimated to be ±30%.

1. Introduction

The aim of the present study is the direct determination of the rate coefficients for the thermal decomposition of acetaldehyde (CH_3CHO) and bimolecular reaction of acetaldehyde with hydrogen atoms at high temperatures. Acetaldehyde is an important intermediate in the combustion of both fossil fuels and biofuels, and the reactions mentioned represent essential steps in the classic Rice−Herzfeld mechanism,[1] which forms an important part of nearly all combustion models.

The main dissociation pathway of acetaldehyde is the C−C bond fission with a bond dissociation energy of 356 kJ mol^{-1} [2]

$$CH_3CHO + M \rightarrow CH_3 + HCO + M \qquad (1)$$

At high temperatures and low radical concentrations, this reaction is followed by the fast and well-characterized[2–6] decomposition of HCO

$$HCO + M \rightarrow H + CO + M \qquad (2)$$

so that both steps can be combined to the overall reaction

$$CH_3CHO + M \rightarrow CH_3 + H + CO + M \qquad (3)$$

because the CH_3 radical does not further decompose under our experimental conditions (average lifetime $\tau(CH_3) > 1$ s at 1500 K and [Ar] $\approx 10^{19}$ cm^{-3}).[2] Elementary steps competing with reaction 1 are the C−H bond fissions

$$CH_3CHO + M \rightarrow CH_3CO + H + M \qquad (4)$$

and

$$CH_3CHO + M \rightarrow CH_2CHO + H + M \qquad (5)$$

which have rather high reaction enthalpies (374 and 471 kJ mol^{-1})[2] and, hence, are comparatively slow. Gupte et al.[7] computed the relative branching fractions of acetaldehyde dissociation reactions other than reaction 1 to be <7% at 2500 K and among these reactions the branching fraction of the H-producing channel with the lowest threshold energy, reaction 4, to be <2%. Therefore, at our experimental conditions (T = 1250−1650 K, see below), reactions 4 and 5 can be safely neglected, and the time dependence of the hydrogen-atom concentration is determined by the progress of reaction 1.

In the past, the thermal decomposition of acetaldehyde was mainly studied at temperatures below 1000 K,[8–14] and only a few kinetic investigations were performed at higher temperatures.[7,15–17]

In 1975, Colket et al.[15] examined the pyrolysis of acetaldehyde in the temperature range 880−1220 K at a pressure of 1 bar in a turbulent flow reactor by detecting the stable products. The experimental results were analyzed in terms of a slightly extended Rice−Herzfeld mechanism, and the following Arrhenius expression for the rate coefficient of reaction 1 was obtained: $k_1 = 10^{15.85 \pm 0.2} \exp[-(41\ 153 \pm 500)\ \text{K}/T]\ \text{s}^{-1}$.

At about the same time, Ernst et al.[16] investigated the thermal decomposition of acetaldehyde in a shock tube over a wide temperature (1350−1650 K) and pressure range (~6, ~25, and ~250 bar) by recording the UV absorption of acetaldehyde at 290.0 nm. From a RRK analysis and by including the results from Colket et al.[15] and Liu and Laidler,[11] the authors deduced the following high-pressure limit for the rate coefficient: $k_{1\infty} = 10^{16.08} \exp[-(41\ 100 \pm 500)\ \text{K}/T]\ \text{s}^{-1}$.

In a recent work, Gupte et al.[7] performed laser-schlieren, shock-tube experiments in the temperature range from 1550 to 2400 K at pressures between 53 and 666 mbar. On the basis of a RRKM/master equation analysis, the temperature and pressure dependence of k_1 was parametrized in terms of a Troe fit[2,18] for 600 K < T < 2500 K and 1 Torr < P < 10^5 Torr.

* To whom correspondence should be addressed. E-mail: Olzmann@chem-bio.uni-karlsruhe.de.

† Present address: Abgaszentrum der Automobilindustrie ADA, c/o Dr. Ing. h.c. F. Porsche AG, Porschestrasse, 71287 Weissach, Germany.

10.1021/jp802030z CCC: $40.75
Published on Web 06/12/2008

Very recently, Yasunaga et al.[17] reported on a shock-tube and modeling study of the acetaldehyde pyrolysis and oxidation (1000 K < T < 1700 K, 1.2 bar < P < 2.8 bar). By simulation of concentration−time profiles for several species with a complex mechanism, rate coefficients were fitted. For reaction 1, the authors obtained $k_1 = 10^{14.78 \pm 0.1} \exp(-39\,800\ \mathrm{K}/T)\ \mathrm{s}^{-1}$.

All the experiments mentioned were performed with comparatively high initial concentrations (>10^{14} cm^{-3}), and the results, therefore, had to be discussed in terms of more or less complex multistep mechanisms. An important reaction in these mechanisms is

$$CH_3CHO + H \rightarrow \text{products} \quad (6)$$

The uncertainty of the rate coefficient for this reaction at elevated temperatures is large, and only estimates or values obtained from fitting to complex mechanisms are available.[2,7,13,17,20] Reaction 6 most likely proceeds via hydrogen abstraction at the carbonyl group,[7,20–24]

$$CH_3CHO + H \rightarrow CH_3CO + H_2 \quad (7)$$

but a hydrogen abstraction at the methyl group[7,17,23]

$$CH_3CHO + H \rightarrow CH_2CHO + H_2 \quad (8)$$

and an addition−elimination channel[24]

$$CH_3CHO + H \rightarrow CH_3 + CH_2O \quad (9)$$

are also possible. The reaction enthalpies are approximately −62, −41, and −14 kJ mol^{-1},[2] respectively. The addition−elimination channel

$$CH_3CHO + H \rightarrow CH_3CH_2 + O \quad (10)$$

mentioned in ref 2 with an endothermicity of 320 kJ mol^{-1} is not competitive.

The acetyl radical, CH_3CO, and vinoxy radical, CH_2CHO, formed in reactions 7 and 8, respectively, were shown at high temperatures to essentially decompose to yield $CH_3 + CO$,[25] where CH_3 as well as CH_2O, which is formed in reaction 9, do not decompose on the time scale of our experiment.[2]

Consequently, at our conditions only negligible amounts of hydrogen atoms are reformed in consecutive steps of the $CH_3CHO + H$ reaction, and the reaction progress can be monitored by detecting H atoms with atom resonance absorption spectrometry (ARAS). The hydrogen atoms in these experiments are produced by the fast thermal decomposition of C_2H_5I via the reaction sequence $C_2H_5I \rightarrow C_2H_5 + I$ and $C_2H_5 \rightarrow C_2H_4 + H$.[26]

The high sensitivity of the ARAS technique allows very low initial concentrations, so that consecutive bimolecular reactions are effectively suppressed. In the current work, we use this advantage to determine the rate coefficients of reactions 1 and 6 directly, that is, without the complications arising from fitting the data to a complex mechanism.

2. Experimental Section

All experiments were performed in a stainless-steel shock tube behind reflected shock waves with argon as the bath gas. The experimental setup has been described previously,[27–29] and only a brief summary is given here.

The shock tube is 7.25 m long and separated by aluminum foil (thickness, 20−100 μm) into a low-pressure section (length, 4.20 m; inner diameter, 10 cm) and a high-pressure section (length, 3.05 m; inner diameter, 9.85 cm). The shock waves were initiated by pressure bursting of the aluminum foil with hydrogen as the driver gas. The test gas in the low-pressure section was argon with a small mole fraction of CH_3CHO (0.5−2.0 ppm) for investigation of reaction 1 or a mixture of CH_3CHO (25−100 ppm) and C_2H_5I (3−6 ppm) for investigation of reaction 6. The shock-wave velocity was measured with pressure transducers, and the postshock conditions were calculated from the initial temperature, pressure, and shock-wave velocity by applying one-dimensional conservation equations and the ideal gas law (see, e.g., ref 30). The detailed reaction conditions are listed in Tables 1 and 2.

The hydrogen-atom concentration was monitored by ARAS at the Lyman α line (121.6 nm). The vacuum−ultraviolet (VUV) radiation was generated in a microwave-discharge lamp consisting of a quartz tube, where a mixture of ~1% H_2 in helium is flown through. An Evenson cavity is mounted to the quartz tube

TABLE 1: Reaction Conditions and Rate Coefficients Obtained for CH_3CHO Decomposition

T (K)	P (bar)	[Ar] (cm^{-3})	$[CH_3CHO]_0$ (cm^{-3})	k_1 (s^{-1})
1270	1.3	7.6×10^{18}	4.8×10^{13}	2.1×10^{1}
1290	1.4	7.9×10^{18}	1.6×10^{13}	3.6×10^{1}
1330	1.3	7.1×10^{18}	4.5×10^{13}	1.1×10^{2}
1330	1.4	7.4×10^{18}	9.2×10^{12}	1.1×10^{2}
1350	1.3	7.1×10^{18}	9.4×10^{12}	1.5×10^{2}
1400	1.4	7.3×10^{18}	4.2×10^{13}	4.8×10^{2}
1410	1.4	7.0×10^{18}	4.4×10^{13}	5.1×10^{2}
1420	1.3	7.6×10^{18}	8.1×10^{12}	7.3×10^{2}
1440	1.2	6.1×10^{18}	3.9×10^{13}	1.2×10^{3}
1450	1.3	6.6×10^{18}	4.2×10^{13}	1.4×10^{3}
1490	1.2	5.9×10^{18}	4.0×10^{12}	2.5×10^{3}
1490	1.3	6.2×10^{18}	7.7×10^{12}	2.2×10^{3}
1520	1.3	6.0×10^{18}	1.2×10^{13}	2.9×10^{3}
1580	1.3	5.7×10^{18}	7.1×10^{12}	1.1×10^{4}
1590	1.3	5.7×10^{18}	7.1×10^{12}	1.1×10^{4}
1600	1.3	5.7×10^{18}	7.5×10^{12}	1.2×10^{4}
1650	1.4	5.9×10^{18}	7.3×10^{12}	1.8×10^{4}
1270	2.9	1.6×10^{19}	2.2×10^{13}	4.9×10^{1}
1290	3.0	1.7×10^{19}	2.1×10^{13}	7.3×10^{1}
1340	2.9	1.6×10^{19}	1.9×10^{13}	2.2×10^{2}
1350	2.9	1.6×10^{19}	1.0×10^{13}	4.0×10^{2}
1400	2.9	1.5×10^{19}	1.9×10^{13}	1.2×10^{3}
1410	2.9	1.5×10^{19}	2.0×10^{13}	9.3×10^{2}
1480	2.9	1.4×10^{19}	1.7×10^{13}	3.6×10^{3}
1500	2.8	1.4×10^{19}	1.8×10^{13}	4.5×10^{3}
1270	5.0	3.0×10^{19}	5.7×10^{13}	1.2×10^{2}
1320	4.5	2.5×10^{19}	1.5×10^{13}	2.5×10^{2}
1340	4.8	2.6×10^{19}	1.8×10^{13}	5.2×10^{2}
1450	4.7	2.3×10^{19}	1.4×10^{13}	4.3×10^{3}
1470	4.9	2.4×10^{19}	1.5×10^{13}	2.9×10^{3}
1490	4.3	2.1×10^{19}	1.3×10^{13}	7.2×10^{3}

TABLE 2: Reaction Conditions and Rate Coefficients Obtained for the $CH_3CHO + H$ Reaction

T (K)	P (bar)	[Ar] (cm^{-3})	$[CH_3CH_2I]_0$ (cm^{-3})	$[CH_3CHO]_0$ (cm^{-3})	k_6 (cm^{-3} s^{-1})
1040	1.4	9.7×10^{18}	2.9×10^{13}	2.5×10^{14}	5.7×10^{12}
1050	1.5	1.0×10^{19}	3.0×10^{13}	2.6×10^{14}	6.0×10^{12}
1060	1.5	1.0×10^{19}	2.9×10^{13}	2.5×10^{14}	5.7×10^{12}
1080	1.4	9.7×10^{18}	2.8×10^{13}	2.3×10^{14}	6.6×10^{12}
1080	1.3	8.8×10^{18}	2.5×10^{13}	2.4×10^{14}	6.8×10^{12}
1090	1.4	9.3×10^{18}	2.7×10^{13}	9.3×10^{14}	5.8×10^{12}
1100	1.3	8.7×10^{18}	5.0×10^{13}	2.5×10^{14}	5.5×10^{12}
1110	1.4	9.2×10^{18}	2.7×10^{13}	2.4×10^{14}	7.7×10^{12}
1110	1.3	9.6×10^{18}	5.1×10^{13}	9.5×10^{14}	6.1×10^{12}
1140	1.4	8.6×10^{18}	2.7×10^{13}	2.4×10^{14}	8.0×10^{12}
1140	1.4	8.7×10^{18}	5.0×10^{13}	9.3×10^{14}	6.6×10^{12}
1150	1.4	9.0×10^{18}	2.6×10^{13}	2.3×10^{14}	7.4×10^{12}
1170	1.4	8.5×10^{18}	2.5×10^{13}	2.2×10^{14}	8.6×10^{12}
1190	1.4	8.4×10^{18}	2.4×10^{13}	2.2×10^{14}	8.9×10^{12}
1200	1.4	8.4×10^{18}	4.8×10^{13}	9.0×10^{14}	8.7×10^{12}
1250	1.4	8.1×10^{18}	2.4×10^{13}	2.1×10^{14}	9.2×10^{12}

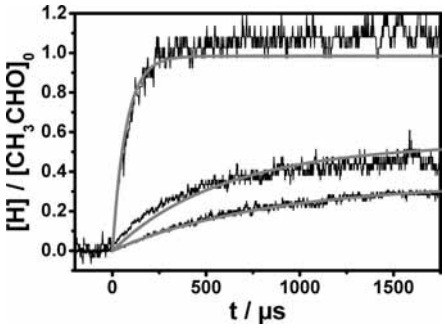

Figure 1. CH_3CHO decomposition. Hydrogen-atom time profiles at a pressure of 1.4 bar and different temperatures (bottom to top: 1400, 1440, and 1600 K): (black lines) measured; (grey lines) modeled (see text).

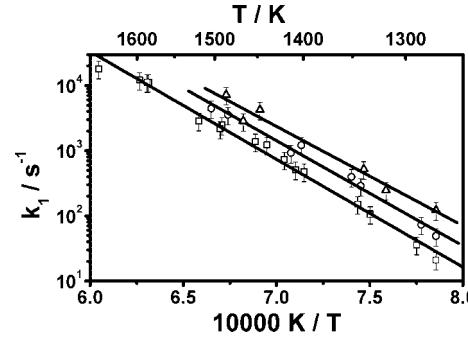

Figure 2. CH_3CHO decomposition. Arrhenius plots of the experimental rate coefficients: (□) $P \approx 1.3$ bar, (○) $P \approx 2.9$ bar, (Δ) $P \approx 4.5$ bar.

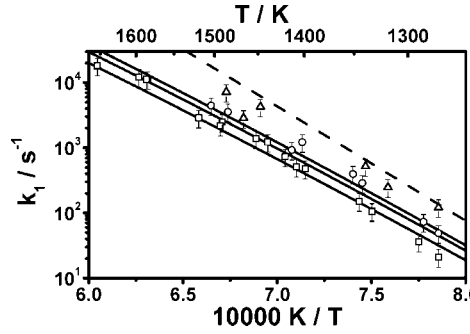

Figure 3. CH_3CHO decomposition. Comparison of our experimental rate coefficients ((□) $P \approx 1.3$ bar, (○) $P \approx 2.9$ bar, (Δ) $P \approx 4.5$ bar) with a parametrization deduced in ref 7 (solid lines from bottom to top: $P = 1.3$, 2.9, and 4.5 bar; dashed line: high-pressure limit).

and coupled to a microwave generator (Muegge), which operates at 2.45 GHz with a typical output power of 100 W. The VUV light is transmitted via MgF_2 windows through the shock tube and after being filtered by a VUV monochromator (Acton Research Corp., Spectra Pro VM-504) detected with a solar-blind photomultiplier (Hamamatsu R1259) and sampled in a storage oscilloscope (Tektronix TDS 540A). The data are further processed in a personal computer.

Calibration experiments with a well-characterized H-atom source have to be done to convert the measured absorbances into concentrations. We have chosen the familiar procedure based on N_2O/H_2 mixtures[30,31] and refer for details again to a recent publication from our laboratory.[28]

The gas mixtures were manometrically prepared in two stainless-steel mixing vessels (100 dm^3), which were evacuated to pressures below 5×10^{-6} mbar before filling. Freshly prepared mixtures were allowed to homogenize for at least 20 h prior to use. Over the whole range of initial concentrations, no systematic variations indicating wall absorption were observed. Moreover, the good agreement between the preset initial concentration of CH_3CHO and the independently determined absolute H-atom concentration at long times in the CH_3CHO dissociation experiments (see Figure 1, $T = 1600$ K) excludes the possibility of larger systematic errors in the initial concentration.

The purity of the gases and chemicals used were as follows: acetaldehyde (Roth) > 99.5%, ethyl iodide (Fluka) > 99.5% (acetaldehyde and ethyl iodide were degassed several times before use), H_2 for calibration (Air-Liquide) > 99.999%, H_2 as driver gas (Air-Liquide) > 99.8%, argon (Air-Liquide) > 99.9999%, and N_2O (Messer Griesheim) 99%.

3. Results and Discussion

3.1. CH_3CHO Decomposition. The acetaldehyde decomposition was studied in the temperature range from 1250 to 1650 K at pressures around 1.3, 2.9, and 4.5 bar. Typical concentration−time profiles of the hydrogen atoms for different temperatures are shown in Figure 1. The increase of the hydrogen-atom concentration is caused by the thermal decomposition of CH_3CHO, and the rate coefficients were determined from the initial slope of the profiles via $k_1 = [CH_3CHO]_0^{-1} \times d[H]/dt$ for $t \rightarrow 0$. At the initial stage of the reaction, bimolecular side reactions can be neglected because of the very low acetaldehyde concentrations. This was verified by varying $[CH_3CHO]_0$ and modeling the hydrogen profiles with a two-step mechanism consisting of reactions 1 and 6 because reaction 6 is the most strongly interfering reaction at early times. For this modeling, the Arrhenius parameters from section 3.2 were used for reaction 6. The results are displayed in Figure 1; it is obvious that small deviations to the measured profiles only occur at longer times and that they have no influence on the determination of k_1. The noticeable difference for the highest temperature in Figure 1 is essentially caused by the steeper calibration curve ([H] vs absorbance, A) for large absorbances. This leads to a higher uncertainty in [H] for a given uncertainty in A as can be realized in Figure 1 also from the lower signal-to-noise ratio. We further note that the small deviation in Figure 1 at early times for $T = 1440$ K is due to the fact that Arrhenius-interpolated rate coefficients were used for the modeling instead of the actually measured values for this temperature.

The rate coefficients obtained from the initial slopes are displayed in Figure 2. Pronounced temperature and pressure dependencies are observed, which can be represented by the following Arrhenius equations.

$$k_1(T, 1.3\ \text{bar}) = 2.9 \times 10^{14} \exp(-38\ 120\text{K}/T)\ \text{s}^{-1} \quad (11)$$

$$k_1(T, 2.9\ \text{bar}) = 2.8 \times 10^{14} \exp(-37\ 170\text{K}/T)\ \text{s}^{-1} \quad (12)$$

$$k_1(T, 4.5\ \text{bar}) = 1.1 \times 10^{14} \exp(-35\ 150\text{K}/T)\ \text{s}^{-1} \quad (13)$$

The maximum error of k_1 is estimated to be ±30%. It is obvious that the rate coefficients are in the falloff region probably not too far from the low-pressure limit, which is in general agreement with earlier experimental[16] and recent theoretical[7] findings. A quantitative comparison of our results with a (corrected[32]) parametrization deduced from statistical rate theory[7] is shown in Figure 3. The agreement in general is reasonable with a certain exception for the highest pressure ($P \approx 4.5$ bar), where our measured rate coefficients somewhat exceed the calculated values and come close to the predicted high-pressure limit. Since the falloff parametrization of ref 7

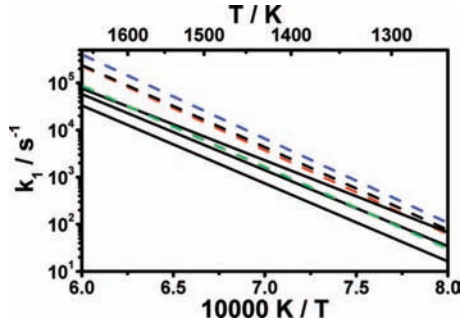

Figure 4. CH_3CHO decomposition. Comparison of the Arrhenius expressions from our experimental data (black solid lines, from bottom to top: $P \approx 1.3$, 2.9, and 4.5 bar) with high-pressure limiting values (dashed lines: green, ref 20; red, ref 16; black, ref 7; blue, ref 2).

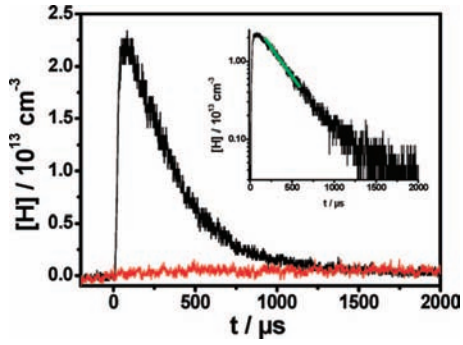

Figure 5. $CH_3CHO + H$ reaction. Hydrogen-atom concentration time profile (black line) and background absorption from acetaldehyde (red line, formally expressed in terms of an equivalent H concentration). Inset: Pseudo-first-order plot and linear fit (green line); $T = 1190$ K, $P = 1.4$ bar, $[C_2H_5I]_0 = 2.4 \times 10^{13}$ cm^{-3}, and $[CH_3CHO]_0 = 2.2 \times 10^{14}$ cm^{-3}.

was accomplished at least in part with respect to the experimental rate coefficients from Ernst et al.,[16] this might also reflect somewhat too low experimental values determined in that work. One should note that the rate coefficients given in ref 16 were obtained by dividing the primarily measured $[CH_3CHO]$ decay rate by 2 to account for the influence of chain processes and the consecutive $CH_3CHO + H$ reaction. As already outlined by Gupte et al.,[7] this correction could be somewhat too large, which would result in too low rate coefficients. This problem is avoided in our work by using much lower initial concentrations.

Another reason for the deviation could be a too low high-pressure limit predicted in ref 7. Different recommendations for the high-pressure limit of k_1 together with the Arrhenius representations of our experimental values are displayed in Figure 4. All curves fall within a narrow range, where we note that there is probably a misprint in the preferred value of ref 2 (pre-exponential factor of 2.1×10^{16} s^{-1} instead of 1.2×10^{16} s^{-1} originally given in ref 16).

Despite the remaining differences, the experimentally determined and calculated rate coefficients $k_1(T,P)$ are in reasonable agreement with slight indications for a somewhat larger high-pressure limiting value.

3.2. $CH_3CHO + H$ Reaction. Reaction of acetaldehyde with hydrogen atoms was studied under pseudo-first-order conditions with respect to CH_3CHO in the temperature range 1040−1240 K at pressures around 1.4 bar. A typical hydrogen-atom time profile is shown in Figure 5. The fast initial increase of the H-atom concentration is caused by the thermal decomposition of ethyl iodide and followed by a decrease due to reaction 6. We note the persistence of a small offset even at longer times, which can be assigned to background absorption from acetaldehyde. This is verified by a control experiment without ethyl iodide in the shock tube but with the same initial concentration of acetaldehyde. The corresponding absorbance (red line in Figure 5) also gives evidence that the thermal decomposition of acetaldehyde can be neglected under our conditions because no additional signal increase due to H atoms is detected after time zero.

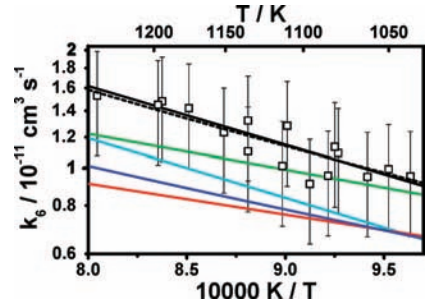

Figure 6. $CH_3CHO + H$ reaction. Arrhenius plot of the rate coefficient: (□) experimental results from this work; (black solid line) linear fit (eq 14); (black dashed line) eq 15; (red line) ref 7; (dark blue line) ref 2; (light blue line) ref 17; (green line) ref 20.

The rate coefficients k_6 were extracted from the linear part of the first-order plots after subtraction of the background absorption (see Figure 5, inset). The results are compiled in Table 2 and displayed in Figure 6. The temperature dependence can be expressed in the following form

$$k_6(T) = 2.6 \times 10^{-10} \exp(-3470\text{K}/T)\ \text{cm}^3\ \text{s}^{-1} \qquad (14)$$

with an estimated maximum error of ±30%.

The temperature range for these experiments is determined at the lower end by a sufficiently fast decomposition of the H-atom precursor C_2H_5I and at the upper end by the incipient decomposition of acetaldehyde. To prove that one can neglect interferences from a possibly too slow decomposition of ethyl iodide, we performed modeling calculations with kinetic data of the ethyl iodide decomposition determined in separate experiments.[33] The deviation of the rate coefficients k_6 obtained as fit parameters from this modeling and those obtained from the first-order plots never exceeded 10%. The latter values are compiled in Table 2 and were used for the parametrization. In an analogous manner the influence of the acetaldehyde decomposition was examined with the kinetic data from section 3.1 and found to have no significant influence on our results for k_6 below a temperature of 1250 K. The pseudo-first-order condition and the absence of interfering bimolecular side reactions were proved by varying the initial acetaldehyde concentration.

To our knowledge, no experimental values of k_6 directly determined in the temperature range of the present work are available. All kinetic data of reaction 6 for temperatures above 500 K published so far were either obtained by fitting to complex mechanisms[7,17] and/or extrapolations from other temperature ranges.[2,20] A comparison is made in Figure 6. The agreement is good with deviations below a factor of 2. If we combine our results with the low-temperature data from refs 23 and 34, which are also used for the recommendation in ref 2, we obtain the following expression for the temperature dependence of k_6 in the range 300−2000 K

$$k_6(T) = 6.6 \times 10^{-18} (T/\text{K})^{2.15} \exp(-800\text{K}/T)\ \text{cm}^3\ \text{s}^{-1} \qquad (15)$$

A comparison with the data from low-temperature experiments is made in Figure 7.

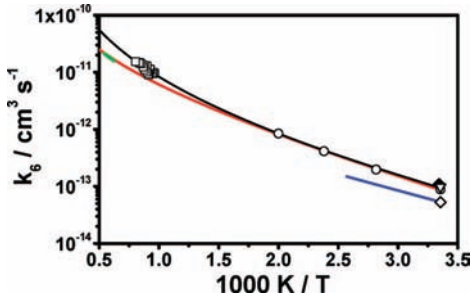

Figure 7. $CH_3CHO + H$ reaction. Comparison with low-temperature data: (□) experimental results from this work; (black solid line) eq 15; (red line) recommendation from ref 2; (green line) ref 13; (blue line) ref 22; (○) ref 23; (▽) ref 34; (◆) ref 35; (◇) ref 36.

The question for the channel branching between reactions 7, 8, 9, and 10 cannot be answered by our experiments. The missing pressure dependence of the rate coefficient k_6 observed[22,23] already at much lower temperatures between 300 and 500 K and pressures up to 530 mbar indicates that a collisional stabilization of the intermediate C_2H_5O radical in reaction 6 is not important. This is true all the more for the higher temperatures of our study. Therefore, we did not perform a pressure-dependent study of reaction 6. In view of the not too different thermodynamic[2] and kinetic[24] data, none of the reaction channels (7, 8, and 9) can be a priori excluded under combustion conditions, and channel branching needs to be examined in future studies.

4. Summary

Rate coefficients for the thermal decomposition of CH_3CHO and the $CH_3CHO + H$ reaction at high temperatures were determined for the first time by directly monitoring H atoms as a product and reactant species, respectively. Due to the low initial concentrations, side reactions were suppressed, and kinetic parameters for these reactions could be obtained without the necessity of complex modeling. In the case of $CH_3CHO + H$, the current work is the first experimental study at temperatures above 500 K. Kinetic parameters of both reactions for use in combustion modeling are provided.

Acknowledgment. Financial support by the Deutsche Forschungsgemeinschaft (SFB 606 "Unsteady Combustion: Transport Phenomena, Chemical Reactions, Technical Systems") is gratefully acknowledged. We thank Jörg Sommerer for help with the experiments.

References and Notes

(1) Rice, F. O.; Herzfeld, K. F. *J. Am. Chem. Soc.* **1934**, *56*, 284.
(2) Baulch, D. L.; Bowman, C. T.; Cobos, C. J.; Cox, R. A.; Just, Th.; Kerr, J. A.; Pilling, M. J.; Stocker, D.; Troe, J.; Tsang, W.; Walker, R. W.; Warnatz, J. *J. Phys. Chem. Ref. Data* **2005**, *34*, 757.
(3) Friedrichs, G.; Herbon, J. T.; Davidson, D. F.; Hanson, R. K. *Phys. Chem. Chem. Phys.* **2002**, *4*, 5778.
(4) Hippler, H.; Krasteva, N.; Striebel, F. *Phys. Chem. Chem. Phys.* **2004**, *6*, 3383.
(5) Krasnoperov, L. *Phys. Chem. Chem. Phys.* **2005**, *7*, 2074.
(6) Hippler, H.; Krasteva, N.; Striebel, F *Phys. Chem. Chem. Phys.* **2005**, *7*, 2077.
(7) Gupte, K. S.; Kiefer, J. H.; Tranter, R. S.; Klippenstein, S. J.; Harding, L. B. *Proc. Combust. Inst.* **2007**, *31*, 167.
(8) Imai, N.; Toyama, O. *Bull. Chem. Soc. Jpn.* **1960**, *33*, 1408.
(9) Trenwith, A. B. *J. Chem. Soc.* **1963**, 4426.
(10) Laidler, K. J.; Liu, M. T. H. *Proc. R. Soc. London A* **1967**, *297*, 365.
(11) Liu, M. T. H.; Laidler, K. J. *Can. J. Chem.* **1967**, *46*, 479.
(12) Bardi, I.; Marta, F. *Acta Phys. Chem.* **1973**, *19*, 227.
(13) Beeley, P.; Griffiths, J. F.; Hunt, B. A.; Williams, A. *Proc. Combust. Inst.* **1977**, *16*, 1013.
(14) Yan, J.-M.; Pan, Y.-Y. *Huaxue Xuebao* **1981**, *39*, 23.
(15) Colket, M. B.; Naegeli, D. W.; Glassman, I. *Int. J. Chem. Kinet.* **1975**, *7*, 223.
(16) Ernst, J.; Spindler, K.; Wagner, H. Gg. *Ber. Bunsen-ges. Phys. Chem.* **1976**, *80*, 645.
(17) Yasunaga, K.; Kubo, S.; Hoshikawa, H.; Kamesawa, T.; Hidaka, Y. *Int. J. Chem. Kinet.* **2008**, *40*, 73.
(18) Troe, J. *J. Phys. Chem.* **1979**, *83*, 114.
(19) Ref. 19 deleted in proof.
(20) Warnatz, J. In *Combustion Chemistry*; Gardiner, W. C., Ed.; Springer: New York, 1984, p. 197.
(21) McKnight, C.; Niki, H.; Weinstock, B. *J. Chem. Phys.* **1967**, *47*, 5219.
(22) Aders, W.-K.; Wagner, H. Gg. *Ber. Bunsen.-Ges. Phys. Chem.* **1973**, *77*, 332.
(23) Whytock, D. A.; Michael, J. V.; Payne, W. A.; Stief, L. J. *J. Chem. Phys.* **1976**, *65*, 4871.
(24) Hippler, H.; Viskolcz, B. *Phys. Chem. Chem. Phys.* **2002**, *4*, 4663.
(25) Senosiain, J. P.; Klippenstein, S. J.; Miller, J. A. *J. Phys. Chem. A* **2006**, *110*, 5772.
(26) Kumaran, S. S.; Su, M.-C.; Lim, K. P.; Michael, J. V. *Proc. Combust. Inst.* **1996**, *26*, 605.
(27) Eng, R. A.; Fittschen, C.; Gebert, A.; Hibomvschi, P.; Hippler, H.; Unterreiner, A.-N. *Proc. Combust. Inst.* **1998**, *27*, 211.
(28) Fernandes, R. X.; Giri, B. R.; Hippler, H.; Kachiani, C.; Striebel, F. *J. Phys. Chem. A* **2005**, *109*, 1063.
(29) Bentz, T.; Giri, B. R.; Hippler, H.; Olzmann, M.; Striebel, F.; Szöri, M. *J. Phys. Chem. A* **2007**, *111*, 3812.
(30) Gardiner, W. C., Jr.; Walker, B. F.; Wakefield, C. B. In *Shock Waves in Chemistry*; Lifshitz, A., Ed.; Marcel Dekker: New York, 1981; p 319.
(31) (a) Appel, D.; Appleton, J. P. *Proc. Combust. Inst.* **1975**, *15*, 701. (b) Just, Th In *Shock Waves in Chemistry*; Lifshitz, A., Ed.;Marcel Dekker: New York, 1981; p 279.
(32) There are misprints in k_0 and F_{cent} for the CH_3CHO decomposition given in ref 7; the correct expressions read as $k_0 = 2.24 \times 10^{57}\ T^{-10.81}$ exp(-95.04 kcal mol^{-1}/RT) cm^3 mol^{-1} s^{-1} and $F_{cent} = 0.601\ T^{-0.162}$ exp ($+1.07$ kcal mol^{-1}/RT) (Klippenstein, S. J. Private communication).
(33) Bentz, T.; Striebel, F.; Olzmann M. To be published.
(34) Michael, J. V.; Lee, J. J. *Chem. Phys. Lett.* **1977**, *51*, 303.
(35) Ohmori, K.; Miyoshi, A.; Matsui, H.; Washida, N. *J. Phys. Chem.* **1990**, *94*, 3253.
(36) Slemr, F.; Warneck, P. *Ber. Bunsen-ges. Phys. Chem.* **1975**, *79*, 152.

JP802030Z